

Supporting Information

Monoclinic VO₂(D) hollow nanospheres with super-long cycle life for aqueous zinc ion batteries

Experimental Section

Preparation of vanadyl oxalate precursor: 3.56 g of oxalic acid (C₂H₂O₄·2H₂O) was dissolved in 100 mL deionized water to form a transparent solution. Then, 2.0 g of commercial V₂O₅ powder was added to the above solution, and the mixture was stirred at 60 °C for a certain time. The color of solution transformed from yellow to green and then blue, suggesting V⁵⁺ was reduced to V⁴⁺. Finally, the blue solution was dried in an air oven at 75 °C for 2 days to obtain the vanadyl oxalate precursor.

Preparation of VO₂(D) hollow nanospheres: 60 mg of vanadyl oxalate precursor obtained above was dispersed into the mixed solvent of CH₃OH (48 mL) and H₂O (12 mL). After completely dissolution, the resulting solution was transferred into a 100 mL Teflon-sealed autoclave, and heated at 200 °C for 24 h. After cooling down to room temperature naturally, the produced precipitates were collected by filtration, and washed with deionized water and absolute ethanol several times. Finally, the product was dried in vacuum at 60 °C for 12 h.

Material characterizations: Crystallographic phases of samples were measured by X-ray power diffraction (D-500, Siemens) using Cu K α radiation. The

morphologies of the products were tested by scanning electron microscope (SEM, JSM-6360LV) and transmission electron microscope (TEM, JEM-2100F). X-ray photoelectron spectroscopic (XPS) was performed on Phi Quantum 2000 spectrophotometer with Al K α radiation for verifying the element valence state.

Electrochemical characterizations: Electrochemical measurements were conducted using CR2025 coin cell. The cathode was prepared by pressing a mixture of 70 wt.% active material, 20 wt.% super P and 10 wt.% PTFE onto titanium mesh, the mass loading was about 1.2-1.5 mg cm⁻² except that in Fig. 5b and 5c (2.5-2.8 mg cm⁻²). Zn metal foil was used as the anode, and 3 M ZnSO₄ aqueous solution as electrolyte. The charge-discharge cycles and rate performance were tested on Neware battery-testing instrument. The cyclic voltammetry (CV, voltage range: 0.2-1.5 V) and electrochemical impedance spectroscopy (EIS) tests were carried out on CHI 660E electrochemical workstation. The EIS were performed in a frequency range of 10⁻² to 10⁵ Hz with an amplitude of 5 mV.

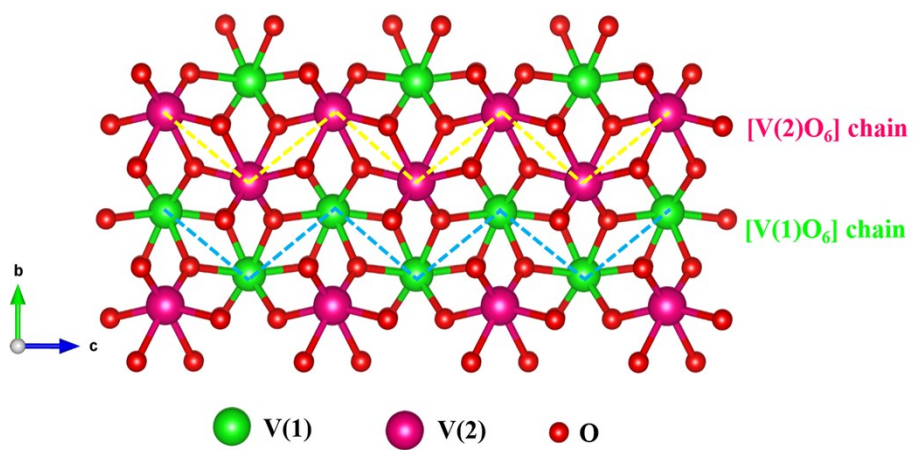


Fig. S1 The crystal structure of monoclinic $\text{VO}_2(\text{D})$.

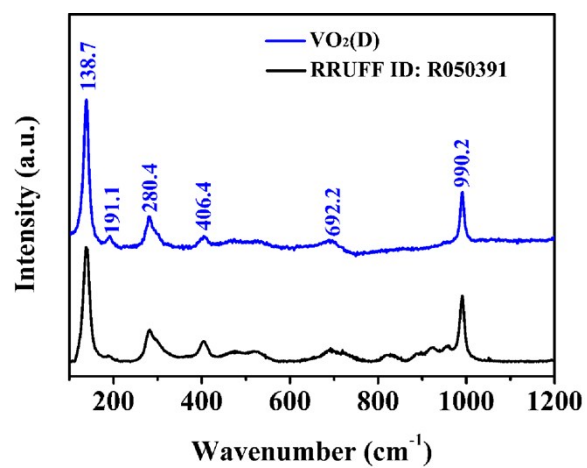


Fig. S2 Raman spectrum of $\text{VO}_2(\text{D})$.

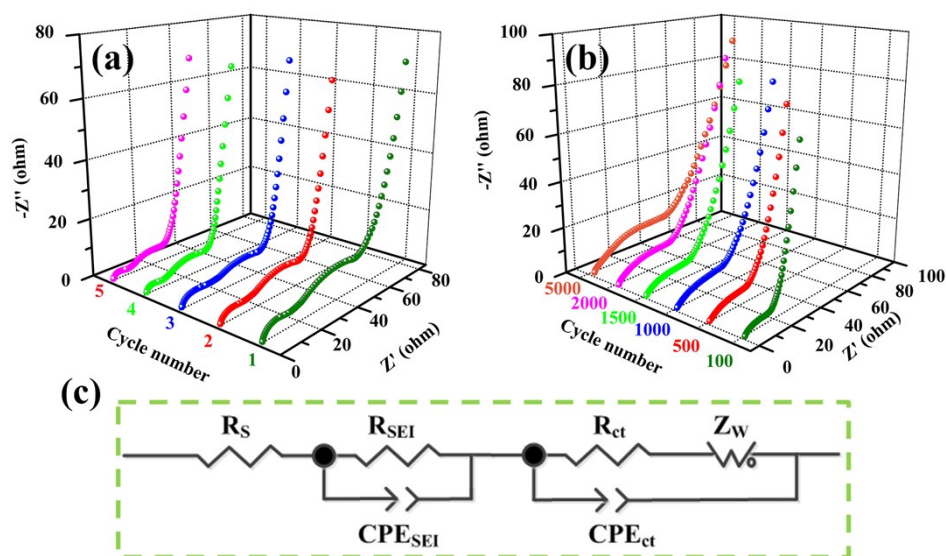


Fig. S3 (a,b) The EIS spectra of the assembled Zn/VO₂(D) battery after different cycles, among which the current density during the cycling was controlled at (a) 0.1 A g⁻¹ and (b) 10 A g⁻¹. (c) The equivalent circuit diagram that can be used to model these EIS spectra.

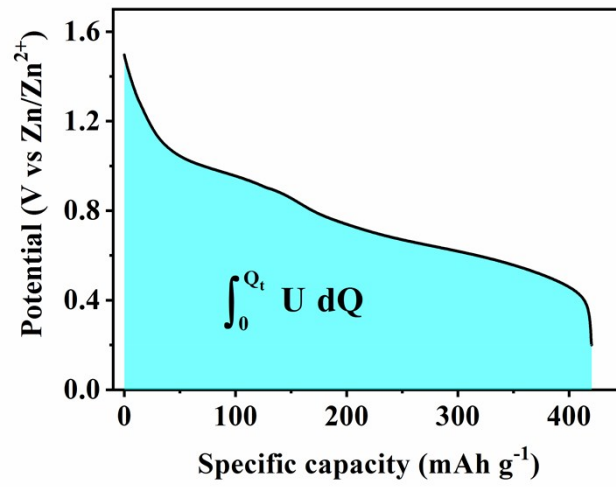


Fig. S4 Discharge curve in the 5th cycle at 0.1 A g⁻¹.

The average discharge voltage is calculated as following [1]:

$$\bar{U} = \frac{1}{Q_t} \int_0^{Q_t} U dQ \quad (1)$$

where U and Q are the potential and the discharge capacity respectively, and Q_t is the total capacity.

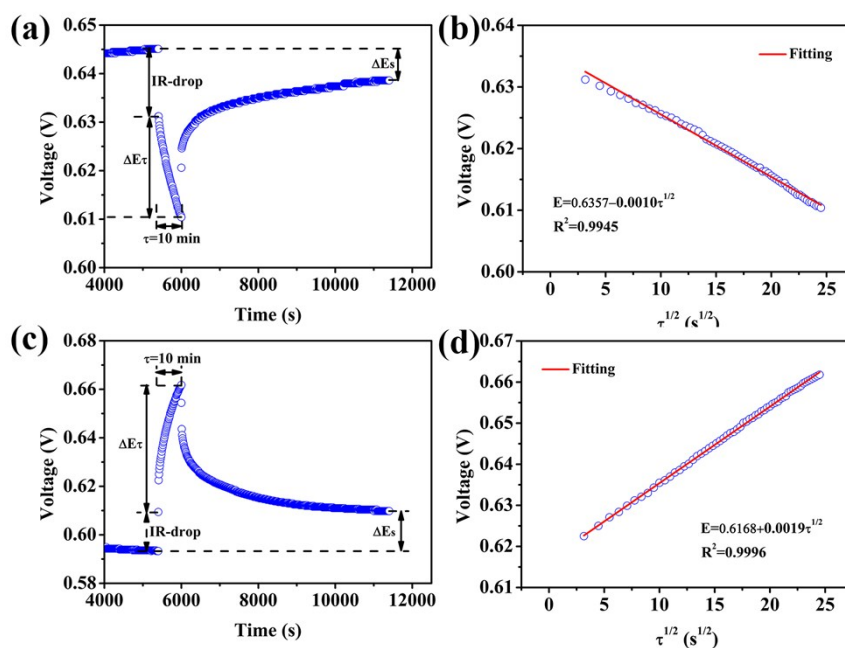


Fig. S5 E vs. t profiles of VO₂(D) electrode for a single GITT and linear behavior of the transient voltage changes E vs. $\tau^{1/2}$ during the discharge (a,b) and the charge (c,d) process.

Detailed test process: prior to GITT measurement, the assembled cells were charged/discharged at 0.1 A g⁻¹ for 5 cycles to activate the battery. In GITT test, the cell was charged or discharged with a test current density of 0.05 A g⁻¹ for an interval of 10 min, followed by an open circuit stand for 90 min, allowing the cell voltage to relax to its steady-state value. The procedure was repeated until the battery reached to the cut off voltage (1.5 or 0.2 V).

Detailed calculation method: considering the linear relationship between transient voltage changes E vs. $\tau^{1/2}$ (Fig. S5b and S5d), the diffusion coefficient of Zn²⁺ can be calculated by the simplified equation [2,3]:

$$D_{Zn} = \frac{4}{\pi\tau} \left(\frac{m_B v_m}{M_B S} \right)^2 \left(\frac{\Delta E_s}{\Delta E_\tau} \right)^2 \quad (1)$$

Where, D_{Zn} ($\text{cm}^2 \text{ s}^{-1}$) is the chemical diffusion coefficient of Zn^{2+} , τ (s) is the pulse duration of constant current, m_B (g), M_B (g mol^{-1}), and v_m ($\text{cm}^3 \text{ mol}^{-1}$) correspond to the quality, molar mass, and molar volume of the active material, respectively, S (cm^2) is the contacting area of electrode with electrolyte (taken as the geometric area of electrode for better comparison with literatures), ΔE_s is the voltage change of the termination voltage of two adjacent relaxation steps, ΔE_τ is the voltage difference during the current pulse subtracting the IR drop.

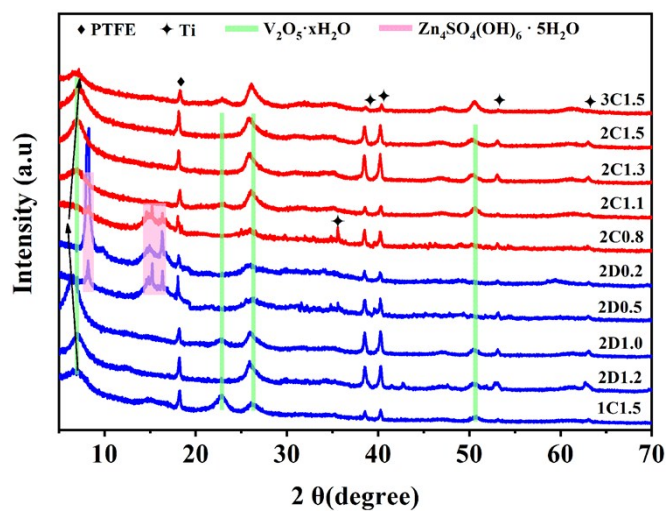


Fig. S6 Ex-situ XRD patterns of $\text{VO}_2(\text{D})$ collected in the second cycle at various discharged/charged states.

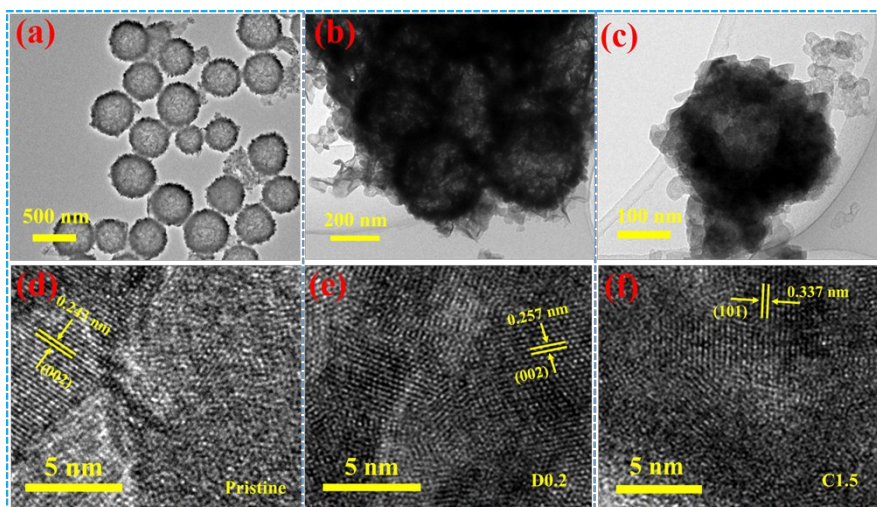


Fig. S7 TEM and HRTEM images of the VO₂(D) electrodes in pristine (a, d), fully discharged (b, e), and charged states (c, f).

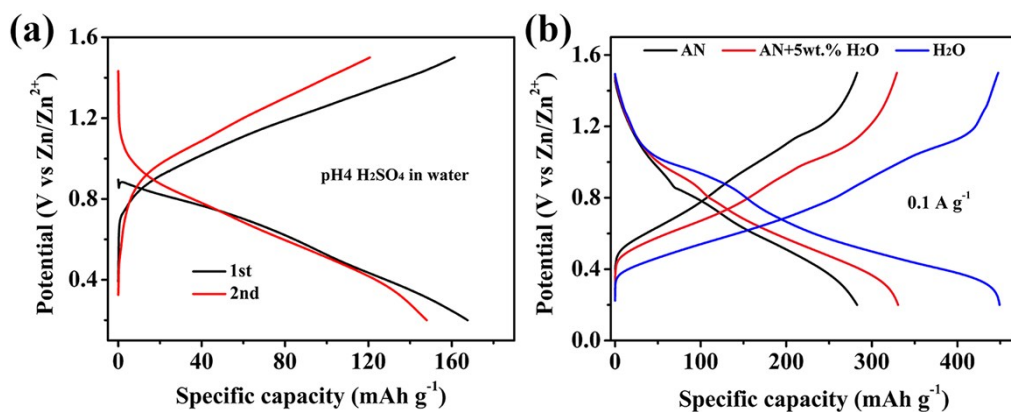


Fig. S8 Galvanostatic discharge/charge curves of VO₂(D) in (a) pH 4 H₂SO₄ electrolyte and (b) 0.1 M Zn(CF₃SO₃)₂ electrolytes with different water content.

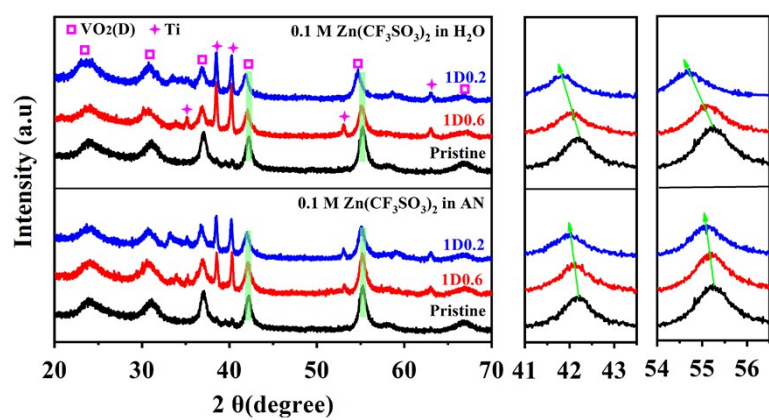


Fig. S9 Ex-situ XRD patterns for VO₂(D) cycled in 0.1 M Zn(CF₃SO₃)₂ electrolytes with pure AN and pure H₂O.

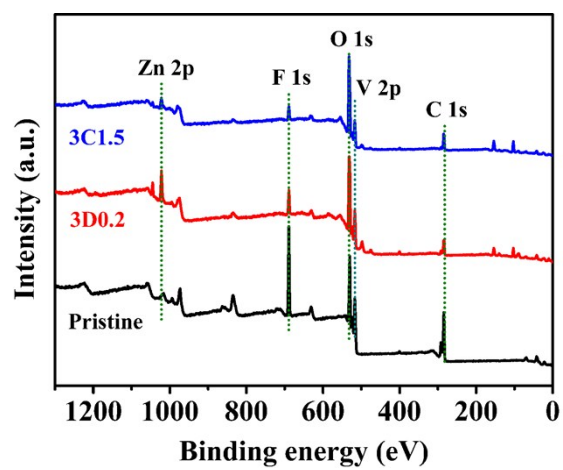


Fig. S10 XPS patterns of VO₂(D) collected in pristine and fully discharged/charged states.

Table S1 Comparison of electrochemical performance of the VO₂(D) electrodes with previously reported vanadium based oxides cathode for ZIBs.

Cathode	Electrolyte	Rate capability	Cycling performance	Ref.
Zn _{0.25} V ₂ O ₅ ·nH ₂ O	1M ZnSO ₄	300/0.3; 260/2.4	211/81%/2.4/1000	[4]
Na ₃ V ₂ (PO ₄) ₃	0.5M Zn(AC) ₂	97/0.05; 58/1	72/74%/0.05/100	[5]
LiV ₃ O ₈	1M ZnSO ₄	256/0.016; 29/1.67	150/75%/0.133/65	[6]
H ₂ V ₃ O ₈	3M Zn(CF ₃ SO ₃) ₂	423.8/0.1; 113.9/5	136.1/94.3%/5/1000	[7]
VS ₂	1M ZnSO ₄	190.3/0.05; 115.5/2	110.9/98%/0.5/200	[8]
Zn ₃ V ₂ O ₇ (OH) ₂ ·2H ₂ O	1M ZnSO ₄	213/0.05; 76/3	101/68%/0.2/300	[9]
V ₂ O ₅ ·nH ₂ O	3M Zn(CF ₃ SO ₃) ₂	372/0.3; 319/15	~213/71%/6/900	[10]
K ₂ V ₆ O ₁₆ ·2.7H ₂ O	ZnSO ₄	239.2/0.1; 178.0/6	154/82%/6/500	[11]
LVO-250	2M ZnSO ₄	470/0.5; 170/10	192/-/10/1000	[12]
(NH ₄) ₂ V ₁₀ O ₂₅ ·8H ₂ O	3M Zn(CF ₃ SO ₃) ₂	228.8/0.1; 123.6/5	~111/90.1%/5/5000	[13]
Na _{0.33} V ₂ O ₅	3M Zn(CF ₃ SO ₃) ₂	367.1/0.1; 96.4/2	218.4/93%/1.0/1000	[14]
VO ₂ (B)	3M Zn(CF ₃ SO ₃) ₂	274/0.1; 133/10	105/79.0%/10/10000	[15]
VO ₂ (B)	3M Zn(CF ₃ SO ₃) ₂	357/0.043; 171/51.2	250/91.2%/0.85/300	[16]
	2M ZnSO ₄	-	~50/15%/0.043/50	
VO ₂ (D)	3M ZnSO ₄	442/0.1; 200/20	298/81%/3/1200	This
			116/48.3%/15/20000	work

Explanation of the above data implications: take the first Zn_{0.25}V₂O₅·nH₂O as an example, i) Rate capability, 300/0.3; 260/2.4 present that 300 mAh g⁻¹ at 0.3 A g⁻¹, and 260 mAh g⁻¹ at a high rate of 2.4 A g⁻¹; ii) Cycling performance, 211/81%/2.4/1000 present that 211 mAh g⁻¹ (capacity retention of 81%) was retained at 2.4 A g⁻¹ after 1000 cycles.

References

- [1] H.G. Qin, Z.H. Yang, L.L. Chen, X. Chen, L.M. Wang, A high-rate aqueous rechargeable zinc ion battery based on the VS₄@rGO nanocomposite, *J. Mater. Chem. A* 6 (2018) 23757-23765. <https://doi.org/10.1039/c8ta08133f>.
- [2] W. Li, K.L. Wang, S.J. Cheng, K. Jiang, A long-life aqueous Zn-ion battery based on Na₃V₂(PO₄)₂F₃ cathode, *Energy Storage Mater.* 15 (2018) 14–21. <https://doi.org/10.1016/j.ensm.2018.03.003>.
- [3] N. Zhang, F.Y. Cheng, Y.C. Liu, Q. Zhao, K.X. Lei, C.C. Chen, X.S. Liu, J. Chen, Cation-deficient spinel ZnMn₂O₄ cathode in Zn(CF₃SO₃)₂ electrolyte for rechargeable aqueous Zn-ion battery, *J. Am. Chem. Soc.* 138 (2016) 12894–12901. <https://doi.org/10.1021/jacs.6b05958>.
- [4] D. Kundu, B.D. Adams, V. Duffort, S.H. Vajargah, L.F. Nazar, A high-capacity and long-life aqueous rechargeable zinc battery using a metal oxide intercalation cathode, *1* (2016) 16119. <https://doi.org/10.1038/nenergy.2016.119>.
- [5] G.L. Li, Z. Yang, Y. Jiang, C.H. Jin, W. Huang, X.L. Ding, Y.H. Huang, Towards polyvalent ion batteries: A zinc-ion battery based on NASICON structured Na₃V₂(PO₄)₃, *Nano Energy* 25 (2016) 211-217. <http://dx.doi.org/10.1016/j.nanoen.2016.04.051>.
- [6] M.H. Alfaruqi, V. Mathew, J. Song, S. Kim, S. Islam, D.T. Pham, J. Jo, S. Kim, J.P. Baboo, Z.L. Xiu, K.S. Lee, Y.K. Sun, J. Kim, Electrochemical zinc intercalation in lithium vanadium oxide: a high-capacity zinc-ion battery cathode,

Chem. Mater. 29 (2017) 1684–1694.

<http://dx.doi.org/10.1021/acs.chemmater.6b05092>.

- [7] P. He, Y.L. Quan, X. Xu, M.Y. Yan, W. Yang, Q.Y. An, L. He, L.Q. Mai, High-performance aqueous zinc-ion battery based on layered $\text{H}_2\text{V}_3\text{O}_8$ nanowire cathode, *Small* 13 (2017) 1702551. <https://doi.org/10.1002/sml.201702551>.
- [8] P. He, M.Y. Yan, G.B. Zhang, R.M. Sun, L.N. Chen, Q.Y. An, L.Q. Mai, Layered VS_2 nanosheet-based aqueous Zn ion battery cathode, *Adv. Energy Mater.* 7 (2017) 1601920. <https://doi.org/10.1002/aenm.201601920>.
- [9] C. Xia, J. Guo, Y.J. Lei, H.F. Liang, C. Zhao, H.N. Alshareef, Rechargeable aqueous zinc-ion battery based on porous framework zinc pyrovanadate intercalation cathode, *Adv. Mater.* 30 (2017) 1705580. <https://doi.org/10.1002/adma.201705580>.
- [10] M.Y. Yan, P. He, Y. Chen, S.Y. Wang, Q.L. Wei, K.N. Zhao, X. Xu, Q.Y. An, Y. Shuang, Y.Y. Shao, K.T. Mueller, L.Q. Mai, J. Liu, J.H. Yang, Water-lubricated intercalation in $\text{V}_2\text{O}_5 \cdot n\text{H}_2\text{O}$ for high-capacity and high-rate aqueous rechargeable zinc batteries, *Adv. Mater.* 30 (2018) 1703725. <https://doi.org/10.1002/adma.201703725>.
- [11] B. Sambandam, V. Soundharrajan, S. Kim, M.H. Alfaruqi, J. Jo, S. Kim, V. Mathew, Y.K. Sun, J. Kim, $\text{K}_2\text{V}_6\text{O}_{16} \cdot 2.7\text{H}_2\text{O}$ nanorod cathode: an advanced intercalation system for high energy aqueous rechargeable Zn-ion batteries, *J. Mater. Chem. A* 6 (2018) 15530–15539. <https://doi.org/10.1039/c8ta02018c>.
- [12] Y.Q. Yang, Y. Tang, G.Z. Fang, L.T. Shan, J.S. Guo, W.Y. Zhang, C. Wang,

- L.B. Wang, J. Zhou, S.Q. Liang, Li⁺ intercalated V₂O₅·nH₂O with enlarged layer spacing and fast ion diffusion as an aqueous zinc-ion battery cathode, *Energy Environ. Sci.* 11 (2018) 3157-3162. <https://doi.org/10.1039/c8ee01651h>.
- [13] T.Y. Wei, Q. Li, G.Z. Yang, C.X. Wang, Highly reversible and long-life cycling aqueous zinc-ion battery based on ultrathin (NH₄)₂V₁₀O₂₅·8H₂O nanobelts, *J. Mater. Chem. A* 6 (2018) 20402-20410. <https://doi.org/10.1039/c8ta06626d>.
- [14] P. He, G.B. Zhang, X.B. Liao, M.Y. Yan, X. Xu, Q.Y. An, J. Liu, L.Q. Mai, Sodium ion stabilized vanadium oxide nanowire cathode for high-performance zinc-ion batteries, *Adv. Energy Mater.* 8 (2018) 1702463. <https://doi.org/10.1002/aenm.201702463>.
- [15] T.Y. Wei, Q. Li, G.Z. Yang, C.X. Wang, An electrochemically induced bilayered structure facilitates long-life zinc storage of vanadium dioxide, *J. Mater. Chem. A* 6 (2018) 8006-8012. <https://doi.org/10.1039/c8ta02090f>.
- [16] J.W. Ding, Z.G. Du, L.Q. Gu, B. Li, L.Z. Wang, S.W. Wang, Y.J. Gong, S.B. Yang, Ultrafast Zn²⁺ intercalation and deintercalation in vanadium dioxide, *Adv. Mater.* 30 (2018) 1800762. <https://doi.org/10.1002/adma.201800762>.